JOC The Journal of Organic Chemistry

Article

pubs.acs.org/joc

Stepwise Diels–Alder: More than Just an Oddity? A Computational Mechanistic Study

Mats Linder and Tore Brinck*

Applied Physical Chemistry, KTH Royal Institute of Technology, Teknikringen 30, S-100 44 Stockholm

Supporting Information

ABSTRACT: We have employed hybrid DFT and SCS-MP2 calculations at the SMD-PCM–6-311++G(2d,2p)//6-31+G(d) level to investigate the relationship between three possible channels for forming a Diels–Alder adduct from a highly nucleophilic diene and moderately to highly electrophilic dienophiles. We discuss geometries optimized using the B3LYP and M06-2X functionals with the 6-31+(d) basis set. The transition states and intermediates are characterized on the basis of geometric and electronic properties, and we also address the possibility of predicting detectability of a zwitterionic intermediate based on its relative stability. Our results show that a conventional Diels–Alder transition state conformation yields intermediates in all four investigated cases, but that these are too short-lived to be detected experimentally for the less activated reactants. The stepwise *trans* pathway, beginning with a conjugate addition-like transition state, becomes increasingly competitive with more activated reactants and is indeed favored for the most electrophilic dienophiles. Addition of a *trans* diene leads to a dead-end as the *trans* intermediates have insurmountable rotation barriers that prohibit formation of the second bond, unless another, heterocyclic intermediate is formed. We also show that introduction of a hydrogen bond donating catalyst favors a stepwise pathway even for less activated dienophiles.

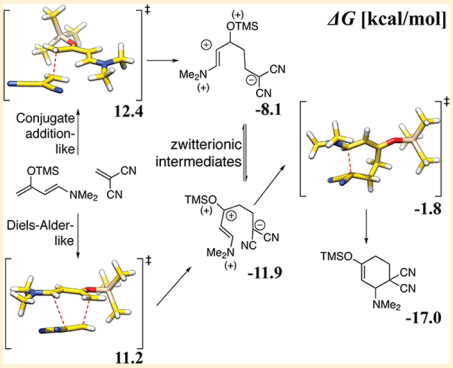

1. INTRODUCTION

As a result of the rich chemistry developed over the years since the seminal paper by Otto Diels and Kurt Alder,[1] many attempts have been made to classify the Diels–Alder reaction according to the overall displacement of electrons and/or transition state geometry.[2] As the available computational resources increase, these issues become increasingly feasible to address *in silico*.[3−5] A large number of recent studies have resulted in several models that describe the mechanistic variety of this seemingly simple reaction. An overview is given in Scheme 1.

One way to classify Diels–Alder reactions is by the amount of charge transfer (CT) in the transition state (TS). This has recently been done for a series of dienophiles reacting with cyclopentadiene,[6] proposing three classes of reactions: non-polar, polar, and ionic. Only a limited number of reactants yield non-polar TSs (Scheme 1a). Most common Diels–Alder reactants fall in the range of polar mechanisms and usually the category given in Scheme 1c, where the TS is asynchronous. Asynchronicity is a property used to describe how "skew" a Diels–Alder TS is, that is, when one incipient bond forms earlier than the other. We will apply a purely geometric meaning to the term to describe a Diels–Alder TS, irrespective of any *a priori* knowledge of whether the reaction is concerted or not. Several computational studies have concluded that TSs of polar Diels–Alder reactions become more asynchronous with more activated reactants and increased CT.[6−9] Asynchronicity can thus be said to be a sign of the extent of nucleophilic addition in the mechanism. The addition can indeed be polar synchronous if the reactants are symmetric, as for example cyclopentadiene with maleic acid anhydride or tetracyanoethylene. This case is not represented in Scheme 1 and will not be considered further in this work. We note in passing that Domingo and colleagues have defined some polar Diels–Alder reactions as being *two-stage*, one-step processes rather than concerted.[6,7] In this work, we will however not differentiate between such flavors of the mechanism and refer to all reactions proceeding without stationary intermediates as "concerted".

A stepwise, diradical pathway (Scheme 1b) as an alternative to the concerted standard TS of non-polar reactants (Scheme 1a) has been investigated carefully but discarded due to a 5 kcal/mol higher activation energy.[2,10] Diradical intermediates are also likely very short-lived in solvent.[11] For normal electron demand (NED) Diels–Alder, reactivity is increased by addition of electron-withdrawing groups (EWGs) to the dienophile and electron-donating groups (EDGs) to the diene, but only in positions *ortho* and *para* to the dienophile substituent (R_2 in Scheme 1). This phenomenon can be explained in terms of local electrophilicity,[12] but also by simple resonance arguments.[8]

Quantum chemical calculations have shown that polar Diels–Alder TSs become more asynchronous as the activation

Received: June 6, 2012
Published: July 10, 2012

   dx.doi.org/10.1021/jo301176t | J. Org. Chem. 2012, 77, 6563–6573

Scheme 1. Four Different Principal Mechanisms of Diels–Alder[a]

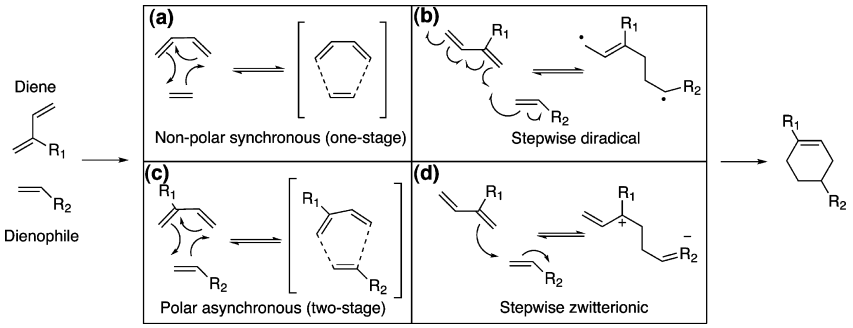

[a]The abundantly implied textbook mechanism is shown in (a) but applies to a small a minority of reactants. The exotic stepwise diradical mechanism is shown in (b). For nearly all cases where R_1,$R_2 \neq H$, the TS is polar and asynchronous, as in (c). The focus of this paper is to investigate the preference for the the mechanism shown in (d), where a conjugate addition leads to a zwitterionic intermediate that yields the Diels–Alder adduct after ring closure.

Scheme 2 Hypothetical Reaction Pathways[a]

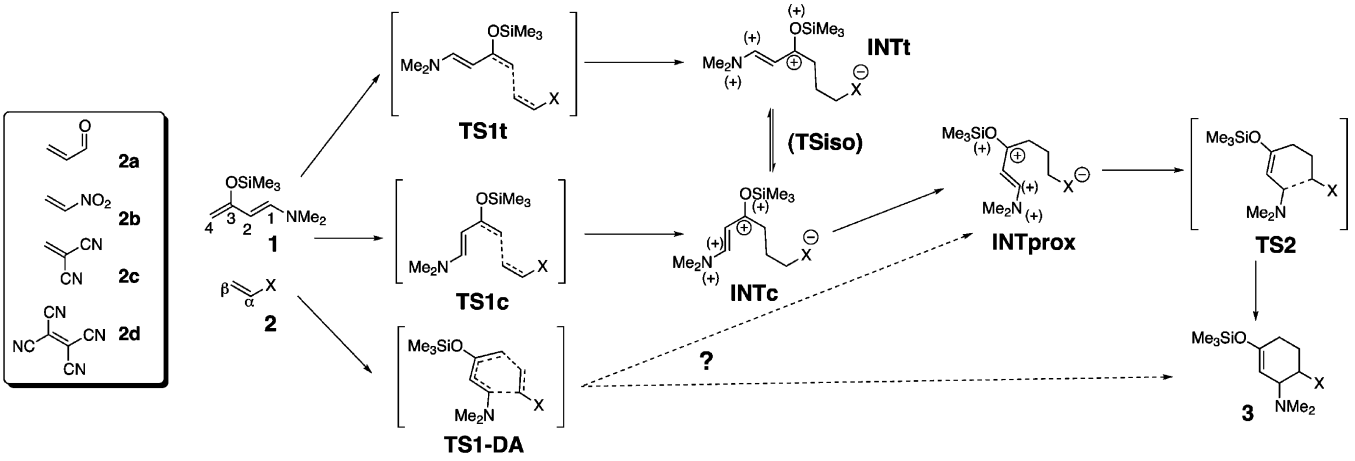

Frontier molecular orbitals and global indices.

	B3LYP/6-31+G(d)				M062X/6-31+G(d)			
	HOMO	LUMO	ω	Δω	HOMO	LUMO	ω	Δω
1	-4.95	-0.25	0.72	- (*N* = 4.78)	-6.22	+0.06	0.76	- (*N* = 4.51)
2a	-7.39	-2.33	2.33	1.61	-9.28	-1.03	1.61	0.85
2b	-8.53	-3.11	3.12	1.70	-10.51	-1.89	2.23	1.47
2c	-8.67	-3.30	3.34	2.62	-10.14	-2.10	2.33	1.57
2d	-9.73	-4.93	5.59	4.87	-10.73	-4.31	4.40	3.64

All values are in eV.

[a]Hypothetical reaction pathways for the cycloaddition of the diene **1** and dienophile **2** to form the cycloadduct **3**. The activated dienophiles **2a–d** are presented in the box. The (+) signs indicate possible loci of positive charge due to resonance stabilization. The inset table displays HOMO and LUMO levels as well as global indices calculated at the 6-31+G(d) level with B3LYP and M06-2X geometries, respectively. The global electrophilicity index ω is calculated using eq 1, and $\Delta\omega = \omega_2 - \omega_1$. The nucleophilicity index N[7] is given for the diene **1**.

barrier decreases and CT increases, and therefore one would intuitively think that there should exist a limit beyond which the concerted mechanism transforms to a stepwise (non-radical) pathway with a zwitterionic intermediate (Scheme 1d). Over the past decade, a multitude of computational studies have explored the possibility of potentially stepwise mechanisms leading to persistent (or at least transient) intermediates. Examples exist of normal electron demand (NED),[13] inverse electron demand (IED),[7] and hetero[7,14] mechanisms. It has also been shown that activating agents, such as Lewis acids and even water,[15] can make an otherwise concerted pathway become stepwise, adding impetus to the argument that a stepwise mechanism is promoted by activation. To further complicate the picture, there are examples of bifurcating reaction coordinates, where the same TS leads to either one of two minima *via* a "valley-ridge intersection point".[16]

Although most studies focus on what happens around a traditional Diels–Alder TS geometry (such as those depicted in Scheme 1a and c), it is quite facile computationally to find TSs and intermediates that differ from the traditional geometry (as the example given in Scheme 1d).[8] To our knowledge, there has been no case reported where the classic, "stacked" Diels–Alder TS geometry (**TS1-DA** in Scheme 2) is disfavored over a conjugate addition-like TS (**TS1t** or **TS1c**), even in presence of a stepwise mechanism and a persistent intermediate.[8,17] However, the increasing number of reports of different mechanistic flavors within Diels–Alder chemistry shows that there is still much to learn about this powerful reaction, as the

dx.doi.org/10.1021/jo301176t | J. Org. Chem. 2012, 77, 6563–6573

paramount work of Woodward and Hoffmann[18] becomes extended to a wider palette of reaction types.

Stepwise Diels–Alder pathways are known experimentally[19] but require cryogenic conditions and very specific reactants that lead to "trapped" intermediates. Recently, experimental detection of a transient stepwise Diels–Alder intermediate was published by Lakhdar et al.[20] In this study, a "super-electrophilic" dienophile, 4,6-dinitrobenzofuroxan, was used. Upon investigating this intriguing system computationally, we found strong support for the stepwise pathway, but we also showed that the lowest-lying intermediate is a heterocyclic adduct. The heterocycle also serves as a relay for *cis-trans* isomerization of the intermediates, connecting the possible TS geometries of the first addition (see Scheme 3a).[17] The barrier of the proposed *cis-trans* isomerization of the zwitterionic intermediates was too high to be viable. An important lesson from our computational study was that the conventional B3LYP functional fails to reproduce the energetic landscape of this type of mechanism, mainly due to the lack of accurate treatment of $\pi \rightarrow \sigma$ transformations.[21]

The demonstration of Lakhdar et al. that a transient intermediate is detectable if it is sufficiently persistent raises important questions regarding the generality of the stepwise mechanism. For example, is it actually present for a wider range of reactants although lack of intermediate stabilization renders detection impossible? In this work, we use Density Functional Theory (DFT) to investigate possible pathways for the Diels–Alder reaction between a highly activated nucleophilic diene and moderately to highly activated electrophilic dienophiles, presented in Scheme 2. We seek to understand if a there exists a transition point in the kinetic preference between a classic conformation and a conjugate addition-like geometry, and we investigate the effect of catalysis. Moreover, given the accessibility of an intermediate state, we address the possibility of experimental detection.

In addition, we compare the quality of B3LYP in DFT calculations with the more recent M06-2X functional.[22,23] Since the potential energy landscape of the challenging systems considered here are expected to be complex and shallow, it is important to use a computational method that is able to predict realistic geometries and energies. We have observed earlier that B3LYP tends to exaggerate asynchronicity in highly polar Diels–Alder reactions, potentially yielding superficial predictions of the relative preference of a stepwise mechanisms.[8,24]

2. COMPUTATIONAL METHODS

The ubiquitous B3LYP[25] hybrid functional has been the workhorse of quantum chemical studies on organic molecules for years.[26] It is well-known, however, that it poorly describes several interactions important for the Diels–Alder reaction. For example, severe problems arise from poor treatment of $\pi \rightarrow \sigma$ transformations[21] and medium to long-range dispersion.[27,28] (See also refs 3 and 26 and references therein.) Such interactions are central in both the reaction complex and transition structure of Diels–Alder reactions, and inaccurate treatment may lead to both erroneous geometries and energies. Moreover, The errors increase in size when applying a larger basis set, mainly due to a reduction in the cancellation of errors.[21,29,30] The most outstanding errors are seen for B3LYP-computed Diels–Alder reaction energies, as will be exemplified below.

The M06-2X hybrid meta-GGA functional[22,23] is constructed to treat dispersion more accurately than older functionals and also does a good job with $\pi \rightarrow \sigma$ reactions such as cycloadditions.[21,31,32] M06-2X represents a more fundamental approach to dispersion treatment than adding empirical corrections, as in e.g. Grimme's DFT-D approach.[27] A recent study by our group concluded that M06-2X performed at least as well as the SCS-MP2[29,33,34] method for reaction energies, barrier heights and intermediates in a Diels–Alder system closely related to the ones considered in this study.[17] B3LYP and standard MP2 gave vastly diverging results, with MP2 giving lower barriers (and reaction energies) relative to M06-2X and SCS-MP2.

Few, albeit a growing number of applied studies have so far used M06-2X for optimization;[35,36] instead B3LYP is still the abundant method of choice. Simón and Goodman recently studied the effect of various DFT functionals on TS geometries[26] and concluded that B3LYP works adequately for optimization in most cases, although there are exceptions. For a comprehensible comparison of geometries, we were therefore prompted to optimize all species considered initially using both B3LYP and M06-2X. The 6-31+G(d)[37] basis set was used for all optimizations. Energies were then calculated at the M06-2X/6-311++(2d,2p) level,[28] using the SMD-PCM[38] continuum model since realistic energies of zwitterions and other species with high dipole moments require proper solvation description. We selected acetone (ε = 20.493) as it represents a moderately polar organic solvent. This is a compromise between more common, non-polar media and highly polar ones such as water, as the goal is to investigate if stepwise intermediates are appreciably persistent in a favorable solvent. All calculations were performed using the Gaussian09 suite.[39] No counterpoise correction was considered as the large basis set used in the energy calculation is expected to reduce the basis set superposition error.[27] M06-2X has been shown to be moderately sensitive to integration grid size, but the default grid used in the Gaussian suite does generally not pose a problem.[40] Instances where a more finely spaced grid has been employed will be noted in the following.

To further characterize each state, we calculated the extent of charge transfer (CT) and Wiberg bond order[41] (BO) from a natural bond orbital (NBO) analysis.[42] The CT descriptor is calculated as the total amount of NBO charge on the dienophile.

3. RESULTS AND DISCUSSION

For each investigated system, the following points on the potential energy surface (PES) were initially considered (see Scheme 2): Free reactants **1** and **2**, a reaction complex **1·2**, a classic Diels–Alder-like TS conformation (**TS1-DA**) as well as conjugate addition-like TSs with the diene in *trans* (**TS1t**) and *cis* (**TS1c**) geometry. Subsequent intermediates (**INTt** and **INTc**) were optimized as well as a proxy intermediate **INTprox**, prearranged to form the second bond through **TS2**. As only a *cis* conformation can lead to a DA product, the rotational barrier **TSiso** between **INTt** and **INTc** was also investigated. The latter calculation was done using unrestricted orbitals in order to detect possible diradical TSs. Finally, the product **3** was optimized. Note that **1·2** is preorganized for the **TS1-DA** channel, although we use it as a proxy for a generic reaction complex.

3.1. Reactants. To create a series of increasingly activated reaction pairs, we have chosen the disubstituted diene **1**, a truncated version of one used by Rawal and co-workers in their work with stereoselective organic Diels–Alder catalysis.[43] As dienophiles, we use the increasingly electrophilic series of acrolein **2a**, nitroethylene **2b**, 1,1-dicyanoethylene **2c**, and tetracyanoethylene **2d**. Activity can be compared using a global electrophilicity index,[44] where the electrophilicity ω is approximated using HOMO and LUMO energies.[45]

$$\omega = \frac{\mu^2}{2\eta} \tag{1}$$

$$\mu \approx \frac{\varepsilon_{\mathrm{HOMO}} + \varepsilon_{\mathrm{LUMO}}}{2} \tag{2}$$

$$\eta \approx \varepsilon_{\mathrm{LUMO}} - \varepsilon_{\mathrm{HOMO}} \tag{3}$$

dx.doi.org/10.1021/jo301176t | J. Org. Chem. 2012, 77, 6563–6573

Table 1. Gas-Phase Free Energies at the M06-2X/6-31+G(d) and B3LYP/6-31+G(d) Levels[a]

	B3LYP				M06-2X			
state	2a	2b	2c	2d	2a	2b	2c	2d
1·2	10.6	7.9	9.8	4.5	7.8	4.8	5.7	0.4
TS1-DA	23.4	18.7	14.2	9.5	21.3	14.3	10.5	0.4
TS1c	29.0	23.2	15.9	11.5	28.1	24.0	14.0	5.8
TS1t	27.3	21.4	14.6	10.8	25.2	21.0	13.8	4.7
INTc	25.9	23.7	10.8	7.5	25.6	24.7	7.6	−4.2
INTt	26.0	19.9	12.1	9.5	23.1	18.3	10.8	0.7
TSiso[b]	43.6	41.5	35.0	35.2	42.0	36.8	32.5	24.9
INTprox	19.7	10.6	3.0	5.0	14.8	2.9	−4.1	−10.8
TS2	18.5	11.5	7.5	10.0	12.3	3.2	−3.1	−8.4
3	−4.4	−10.6	−2.9	3.3	−20.3	−27.7	−22.1	−22.7

[a]All energies are given in kcal/mol. [b]Only approximate **TSiso** states could be found by applying geometric constraints.

Table 2. Solution M06-2X/6-311++G(2d,2p) Free Energies on B3LYP and M06-2X Gas-Phase Geometries[a]

	B3LYP opt				M06-2X opt				$\Delta\Delta G_{\text{M06-2X–B3LYP}}$[b]			
state	2a	2b	2c	2d	2a	2b	2c	2d	2a	2b	2c	2d
1·2	11.3	7.9	6.1	0.8	6.7	7.5	7.9	0.4	−4.6	−0.4	+1.7	−0.3
TS1-DA	21.8	14.9	9.8	−2.6	21.2	15.4	11.2	1.2	−0.6	+0.5	+1.4	+3.7
TS1c	26.0	17.4	13.1	−2.2	26.8	19.3	12.4	1.9	+0.8	+1.8	−0.7	+4.0
TS1t	24.9	16.6	8.7	−4.8	24.5	16.9	6.9	−1.1	−0.4	+0.3	−1.8	+3.7
INTc	17.4	2.1	−6.2	−18.7	13.9	0.6	−8.1	−18.7	−1.6	−1.6	−1.9	0.0
INTt	15.3	2.4	−8.0	−19.5	12.9	1.3	−9.2	−19.0	−2.4	−1.1	−1.2	+0.5
TSiso[c]	35.9	26.3	17.0	6.4	39.5	30.5	14.3	13.7	+3.6	+4.2	−2.7	+7.3
INTprox	10.9	−3.1	−11.3	−18.9	8.3	−3.9	−11.9	−19.0	−2.6	−0.8	−0.6	−0.1
TS2	12.7	1.5	−2.2	−13.8	11.5	−1.0	−1.8	−11.1	−1.2	−2.5	+0.4	+2.8
3	−13.6	−19.0	−13.8	−16.2	−16.9	−24.3	−17.0	−18.9	−3.3	−5.3	−3.3	−2.7

[a]All energies were calculated using the SMD-PCM solvent model (acetone) and are given in kcal/mol. Thermodynamic corrections have been calculated at the level of optimization. A 1.89 kcal/mol correction is included for the standard state 1 M. [b]Difference between M06-2X and B3LYP geometries. [c]Only approximate **TSiso** states could be found by applying geometric constraints.

The difference in global electrophilicity ($\Delta\omega$) has been used by Domingo and others as a descriptor for the amount of activation in Diels–Alder reactions.[6,7,46,47] Domingo has also introduced a nucleophilicity index N, which is defined as $N = \varepsilon^{\text{Nu}}_{\text{HOMO}} - \varepsilon^{\mathbf{2d}}_{\text{HOMO}}$.[6,7] It is thus essentially a translation of the nucleophile's HOMO energy. We will mention the utility of $\Delta\omega$ in the context of stepwise Diels–Alder when appropriate.

Until now, most studies on Diels–Alder reactivity have employed relatively small basis sets, mainly 6-31G(d), making it quite straightforward to compare different studies using a common descriptor. Correlation with the global electrophilicity scale becomes more problematic with the use of larger basis sets and different functionals, so we will use the indices computed using the smaller basis set. For comparison, all HOMO and LUMO as well as global indices are given in Table 1 for both B3LYP and M06-2X geometries. **2d** is predicted to be the most reactive dienophile using either ω or the LUMO level as expected, while **2a** is predicted to be the least reactive. **2b** and **2c**, on the other hand, have similar values of both ω and LUMO energy.

3.2. Energies. It was straightforward to optimize all species using standard gas-phase calculations, which in itself indicates that the zwitterionic intermediates have well-defined minima on the PES. (A comparison to solvent-optimized geometries is briefly discussed below.) 6-31+G(d) gas-phase free energies of the states indicated in Table 2 are given for both the B3LYP and M06-2X geometries in Table 1. The energies of all intermediates are, as expected, high compared to the surrounding barriers (**TS1** and **TS2**), since no solvent continuum is present to stabilize the zwitterion. We therefore focus the discussion on the M06-2X/6-311++G(2d,2p) level, for which the solvent-corrected energies are given in Table 2, and refer back to Table 1 as needed. For both levels of theory, potential energy surfaces without thermodynamic corrections are provided in the Supporting Information.

As anticipated, the activation energies decrease as we move down the series of dienophiles. Of the two possible stepwise TS conformations, **TSt** is consequently favored over **TSc**. Furthermore, **TSt** approaches **TS1-DA** when going from **2a** to **2b** and becomes the lowest TS for **2c** and **2d**. A similar trend is seen for the intermediate states; **INTc** and **INTt** of **1** + **2a** are too unstable to be present to any extend during a reaction, while the **1** + **2d** zwitterion appears to be as stable as the cycloadduct. Entropy contributions, given in the Supporting Information, show that there are only small differences between the three channels.

The **INTprox**–**TS2** barrier is 1.8, 4.7, 9.1, and 5.5 for the B3LYP geometries, and 3.2, 3.0, 10.1, and 7.9 for the M06-2X geometries. Taking the difference between the second and (lowest) first barrier, we obtain energy differences of −20.0, −10.2, +0.3, +9.8 and −18.0, −12.4, +3.2 and +9.0 for B3LYP and M06-2X geometries, respectively. Hence, the rate-determining step transitions from being the initial addition to the second C–C bond formation along a stepwise pathway. It remains to be shown (see below) whether **TS1-DA** proceeds to **INTprox** or concertedly to the product **3**. Regardless, however, the small second barriers in the **2a** and **2b** systems make clear

dx.doi.org/10.1021/jo301176t | J. Org. Chem. 2012, 77, 6563–6573

Table 3. Additional 6-311++G(2d,2p) Single-Point Energies on the B3LYP and M06-2X Optimized 1 + 2c System[a]

	B3LYP opt; sp B3LYP			M06-2X opt					
				sp B3LYP			sp SCS-MP2		
state	ΔE_{SCF}	ΔG	$\Delta\Delta E^b$	ΔE_{SCF}	ΔG	$\Delta\Delta E^b$	ΔE_{MP2}	ΔG	$\Delta\Delta E^b$
1·2	2.4	10.2	+4.1	6.3	17.6	+10.0	−3.2	8.1	+1.0
TS1-DA	1.4	12.8	+3.0	5.3	19.6	+8.4	0.4	14.7	+3.5
TS1c	2.0	13.5	+0.4	3.0	15.7	+3.3	4.8	17.5	+5.1
TS1t	−2.8	8.2	−0.6	−2.6	9.5	+2.6	0.6	12.7	+5.8
INTc	−17.3	−3.6	+2.6	−16.2	−1.1	+6.9	−17.4	−2.4	+5.7
INTt	−19.4	−6.5	+1.5	−16.4	−2.4	+6.8	−17.0	−3.0	+6.2
TSiso[b]	8.0	20.0	+3.5	9.2	22.6	+8.3	10.5	23.9	+9.6
INTprox	−18.8	−4.6	+6.7	−18.6	−3.4	+8.5	−23.6	−8.4	+3.5
TS2	−7.8	7.6	+9.8	−7.6	9.0	+10.8	−18.0	−1.5	+0.3
3	−14.8	2.3	+16.1	−13.9	4.0	+21.0	−37.1	−19.2	−2.2

[a]All energies were calculated using the SMD-PCM solvent model (acetone) and are given in kcal/mol. Thermodynamic corrections have been calculated at the level of optimization. A 1.89 kcal/mol correction is included for the standard state 1 M. [b]Difference with respect to the M06-2X/6-311++G(2d,2p) energies of the optimized structures. [c]Only approximate **TSiso** states could be found by applying geometric constraints.

that the intermediates are likely not persistent enough to be traceable by conventional experimental methods.

In order for the product **3** to be formed from **INTt**, there must be a feasible bond rotation of the diene moiety to form **INTc** (see Table 2). Finding a fully relaxed rotational TS proved to be a challenging task, and we had to use geometric constraints to find reasonable transition structures. All **TSiso** energies should therefore be regarded as approximate. Nevertheless, it is clear that the rotation is unfavorable with barriers ranging from 20 to 30 kcal/mol depending on dienophile and method. The energies of **TSiso** with respect to free reactants follow the same trends as the other states, but the relative barriers remain high. An investigation of the spin eigenvalues from the unrestricted optimizations of **TSiso** showed that S^2 = 0 in all cases and hence that there is no diradical character.

The reader will note from Table 2 that there seems to be some instances in the **1** + **2c** and **1** + **2d** systems where the **TS1** energies lie below the reaction complex. This is because the SMD-PCM−6-311++G(2d,2p) PES cannot be completely superimposed on the 6-31+G(d) PES (no "negative" TS appears in Table 1), but also since **1·2** is only an approximate representation of a pre-attack complex for, e.g., **TS1t**. To control how the continuum solvation might influence the geometry and PES, we optimized the **1** + **2c** system at the SMD-PCM−M06-2X/6-31+G(d) level, using the "Ultrafine" grid option, and performed a subsequent 6-311++G(2d,2p) calculation. The resulting energies and geometries, reported in the Supporting Information, are similar at large and do not change the overall position of each state. The main differences are that all TSs are closer in energy and above the reaction complex and that the three intermediates are further stabilized by 3−6 kcal/mol, establishing **INTprox** → **TS2** as the rate-determining step. The importance of solvation for stabilization of the zwitterions can be further illustrated by comparing the solvent-corrected M06-2X/6-311++G(2d,2p) single-point energies in Table 2 with gas-phase energies, which reveals that most of the intermediate stabilization comes from the addition of a solvent model rather than a larger basis set (see the Supporting Information for a more thorough discussion).

The difference in M06-2X/6-311++G(2d,2p) free energies between B3LYP and M06-2X geometries, displayed in the rightmost columns in Table 2, are small in general, consistent with the conclusions of Simón and Goodman.[26] However, they are significant for the charged intermediates and the second barrier, which effectively determine if the mechanism is stepwise or concerted. The largest differences are seen in the products and the **1** + **2d** TSs. We can also compare the two methods by following how the energy landscape differs between the higher level of theory and the optimization level (*cf.* Tables 1 and 2). In general, the differences for the B3LYP geometries are larger, which is expected since with the M06-2X geometries, the large and small basis PESs are more superimposable. The B3LYP reaction coordinate of **1** + **2d** is clearly an outlier, highlighting the requirement of a more accurate method at the optimization stage for the type of reactions considered here.

Is the M06-2X functional adequate for energy predictions? We have previously used SCS-MP2[29,33,34] and obtained results consistent with M06-2X.[17,24] Consequently, we performed SCS-MP2 calculations on the **1** + **2c** system as an internal benchmark of the all-M06-2X protocol. The results are shown in Table 3 together with the B3LYP level for reference. We observe the same relationship between M06-2X and SCS-MP2 as we have reported previously in ref 17; the PES is shifted upward by several kcal/mol, while the internal differences are more or less conserved. The main difference here is a decreased second barrier with respect to M06-2X. Although B3LYP does a fairly good job at reproducing the approximate energy landscape, at least of B3LYP geometries, we note the usual overestimation reaction energies.[29] Importantly, the change in energy of the three TS1 states is reversed with respect to SCS-MP2, indicating that B3LYP overestimates the benefits of charge-transfer and underestimates dispersion. Thus, comparing the reaction pathways using B3LYP yields an artificial preference for the stepwise mechanism.

We conclude this section with stating that the SMD-PCM−M06-2X/6-311++G(2d,2p)//6-31+G(d) protocol employed here seems sufficiently accurate to make predictions on both energies and geometries for the reactions studied here. It will be used and referred to exclusively in the following, if not otherwise indicated.

3.3. Geometries and Descriptors. Molecular geometries are shown in Figure 1 along with calculated CT and BO descriptors. In terms of both charge-transfer and bond order ($BO_{4-\beta}$), we see from Figure 1 that **TS1c** and **TS1t** are later on the reaction coordinate than **TS1-DA**, even when they are energetically favored. In all four instances of **TS1-DA**, $BO_{1-\alpha}$ is small, showing that these TSs correspond to either asynchronous two-stage or potentially stepwise mechanisms. The CT

dx.doi.org/10.1021/jo301176t | J. Org. Chem. 2012, 77, 6563−6573

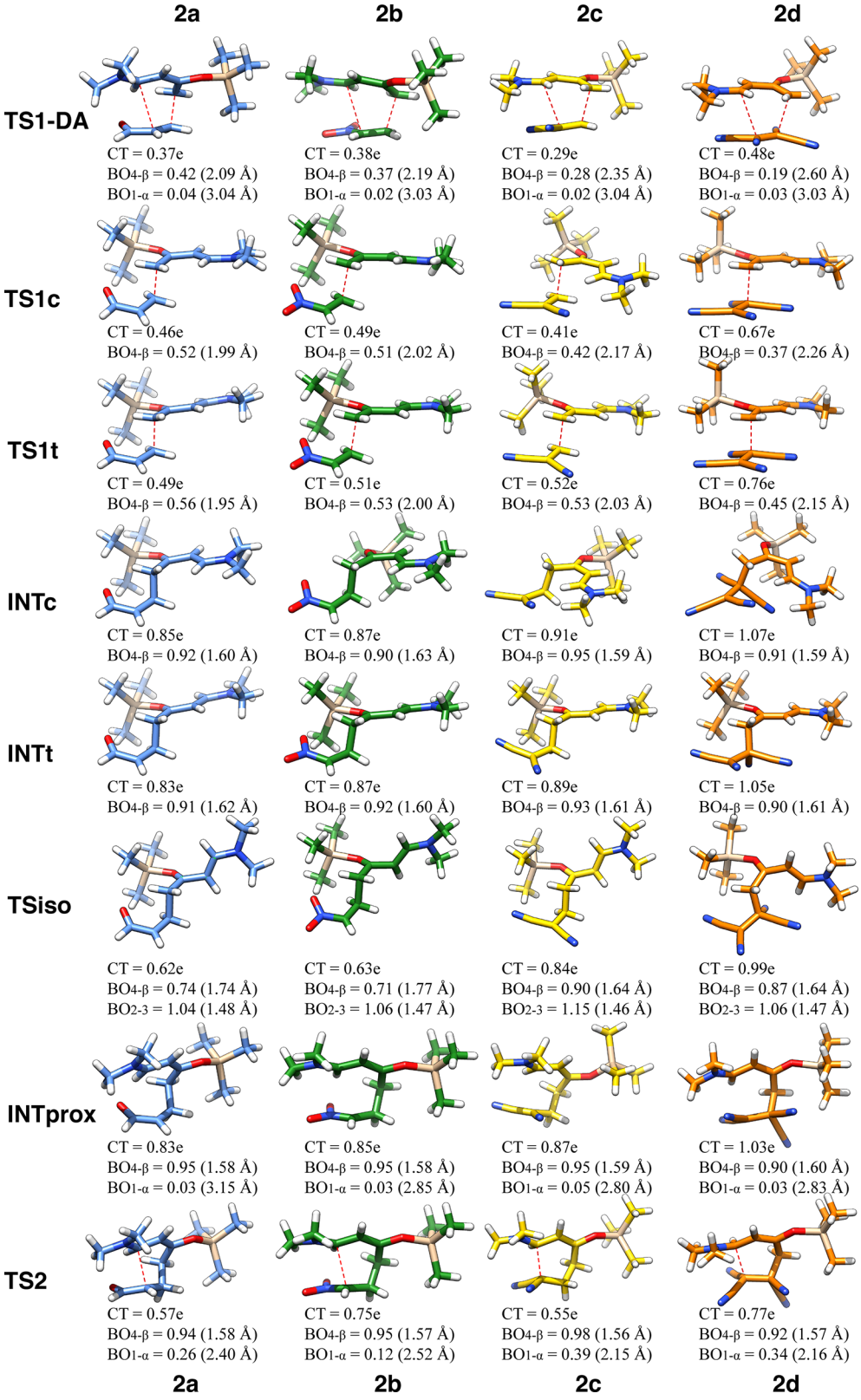

Figure 1. Graphical representations of the investigated states on the M06-2X/6-311++(2d,2p)//M06-2X/6-31+(d) potential energy surface. Charge transfer (CT) and bond order (BO) descriptors are used to characterize them. CT is reported in atomic units. $BO_{4-\beta}$ is the bond formed between the diene C_4 and dienophile C_β, and $BO_{1-\alpha}$ is the C_1-C_α bond order. Atom labeling refers to Scheme 2. Distances in Ångströms are also included.

descriptor clearly shows they are very polar according to the Domingo classification.[6]

The amount of CT increases down the series of dienophiles in both TSs and intermediates, consistent with the increasing electrophilicity. It is close to unity in the intermediates, confirming that they can be regarded as zwitterions. Note that the new carbon−carbon bond lengths (1.58−1.63 Å), are uncommon but known.[48] Since they do not change significantly

dx.doi.org/10.1021/jo301176t | J. Org. Chem. 2012, 77, 6563−6573

down the series, the relative stability of the intermediates is likely to originate from the increased charge transfer to the electrophilic dienophiles. In **TSiso**, the diene−dienophile bond is weakened as the diene carbon acquires more electron density due to electrons being pushed from the rotating bond. As seen from BO_{2-3}, the rotating bond is approximately single, while having bond orders of 1.4−1.6 in the other intermediate states. There is also less charge-transfer character in **TSiso**, contributing to weakening of the diene-dienophile bond. These points explain why *cis-trans* isomerization does not likely take place after the first bond formation and means that **INTt** is apparently a dead-end on the reaction coordinate.

Interestingly, $BO_{1-\alpha}$ in the proxy intermediate **INTprox** is virtually the same as in **TS1-DA**, indicating a delicate difference between a concerted reaction path and a path involving two separate bond-forming events. In all four cases **INTprox** is the most favored intermediate and can be accessed directly from **TS1-DA** or by facile rotation around the newly formed carbon−carbon bond in **INTc**. Finally, in **TS2** the amount of charge transfer decreases as electrons are pushed back from the dienophile into the diene. The second carbon−carbon bond is well underway without any large alterations of the first bond.

From frequency analysis of **TS1-DA**, it is not clear whether the reaction coordinate leads directly to the Diels−Alder adduct or to an intermediate such as **INTprox**. The fact that **TS1-DA** is favored or close to otherwise favored TSs in all four systems and that **INTprox** is the lowest observed intermediate raised the question whether **TS1-DA** leads to **INTprox** or directly to the product, i.e., is this pathway stepwise or concerted? Intrinsic reaction coordinate (IRC)[49] calculations were therefore performed from each **TS1-DA** at both the B3LYP/6-31+G(d) and M06-2X/6-31+G(d) levels (M062X required the "Ultrafine" grid option in Gaussian09 to work). To our surprise, all four species ended up in **INTprox** in the forward direction (Figure S2). Hence, even when the conventional **TS1-DA** channel is favored the reaction proceeds *via* an intermediate. The possibility that the end points found are saddle points on a potential surface bifurcation[16] can be discarded since the frequencies of all **INTprox** species show that these states are true minima on the PES.

We have seen that all **TS1-DA** are geometrically asynchronous and formally conjugate addition-like TSs, but contrary to what is often observed there is a decrease in the relative incipient bond distance with increased activity for the M06-2X geometries of **TS1-DA** (Figure 1). Figure 2 shows an overlay of each **TS1-DA** optimized with the two different functionals. We use $d_\alpha - d_\beta$ as a descriptor of asynchronicity[50] and see that the difference between M06-2X and B3LYP increases with increasing reactivity of dienophiles. The M06-2X geometries become increasingly synchronous due to increasing C_4-C_β distances. This result can attributed to the improved ability of M06-2X to treat dispersion compared to B3LYP, yielding a description of successively earlier TSs. It also means that B3LYP accentuates the charge-transfer character of **TS1-DA**, leading to very asynchronous geometries.

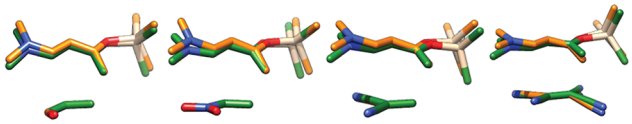

d_α - $d\beta$ (Å)	2a	2b	2c	2d
B3LYP	1.000	1.019	0.983	0.945
M062X	0.951	0.846	0.688	0.457

Figure 2. Overlays of the **TS1-DA** states calculated using B3LYP (orange) and M06-2X (green). Hydrogens are omitted for sake of clarity. The overlays were created by aligning the atoms corresponding to the α-, β-, and carbonyl carbons in **2a**. The $d_\alpha - d_\beta$ difference is used as a measure of asynchronicity, where d_α and d_β represent the C_1-C_α and C_4-C_β distances.

3.4. An Alternative Route to Isomerization. As mentioned in the introduction, we found when studying the stepwise Diels−Alder mechanism of **4** + **5** that the only possible route to *cis-trans* isomerization is *via* a heterocyclic adduct, as shown in Scheme 3a. After cyclization, the C_2-C_3 bond is purely single and facile to rotate.[17] Moreover, we showed that the heterocyclic intermediate (henceforth referred to as **INTcyc**) is in fact more stable than the zwitterionic counterparts, which can be explained by the collapse of charge-separation. It has also been demonstrated that for the Lewis Acid-catalyzed reaction between butadiene and acrolein (**2a**) can proceed *via* a stepwise mechanism with an **INTcyc**-like intermediate, although that pathway is disfavored compared to the regular [4 + 2] channel.[51]

Analogous mechanisms in the present study are easy to deduce, as shown in Scheme 3b. We therefore investigated whether there is an accessible pathway between **INTt** and **INTc** *via* **INTcyct**/ **INTcycc**. We considered only the M06-2X geometries and all calculations were performed as described in the Methods section. The results are summarized in Figure 3, which shows three distinct states. Since we have previously shown that **INTt** → **INTcyct** and **INTc** → **INTcycc** barriers are essentially equivalent, we consider only the former here. We also omit any attempts to find the **INTcycc** → **INTcyct** barriers since they are expected to be only 4−5 kcal/mol.[17]

The results shown in Figure 3 indicate that the heterocyclic adducts **INTcycc** and **INTcyct** are indeed the lowest intermediate states on the PES for **2a** and **2b**. The stabilization is dramatic for **2a** and more modest for **2b**. Corresponding Schiff base intermediates of **2c** and **2d** were too unstable to provide accessible isomerization routes. The cyclization barriers $\Delta\Delta G_{\mathrm{INTt-TScyc}}$ are 6.2 and 2.8 kcal/mol for **2a** and **2b**, respectively. For **2a**, the reverse barrier $\Delta\Delta G_{\mathrm{INTt-TScyc}} \approx 25$ kcal/mol, signaling that **INTcyc** could act as an energy trap. However, for the uncatalyzed reaction, the favored **TS1-DA** pathway means that the product **3** is both kinetically and thermodynamically favored. The corresponding reverse barrier for **2b** is much lower (∼10 kcal/mol), suggesting that formation of **INTcyc** could indeed act as a channel for **INTt**→**INTc** conversion. We note that the **INTcyc** species are formally [2 + 4] cycloadducts, but due to the large charge-transfer involved the two-step pathway is favored.[17]

3.5. An Organocatalyst Increases the Preference for the Stepwise Pathways. Organic catalysis of addition reactions is becoming increasingly popular,[3−5] and numerous cases of Diels−Alder reactions catalyzed by hydrogen bond (H-bond) donors exist in the literature (see Scheme 4a for some examples).[43,52−54] The molecular catalyst generally interacts with the EWG on the dienophile, thereby lowering the LUMO and increasing its electrophilicity. Moreover, TSs and possible intermediates are stabilized since the charge build-up on the EWG strengthens the hydrogen bond to the catalyst.

In this section, we will briefly explore the effect of catalysis on the relative preference for a **TS1-DA**, **TS1c**, and **TS1t**. Since most organic catalysts for this type of reaction are designed to interact with carbonyl groups, we use **2a** together with 4,5-

dx.doi.org/10.1021/jo301176t | J. Org. Chem. 2012, 77, 6563−6573

Scheme 3[a]

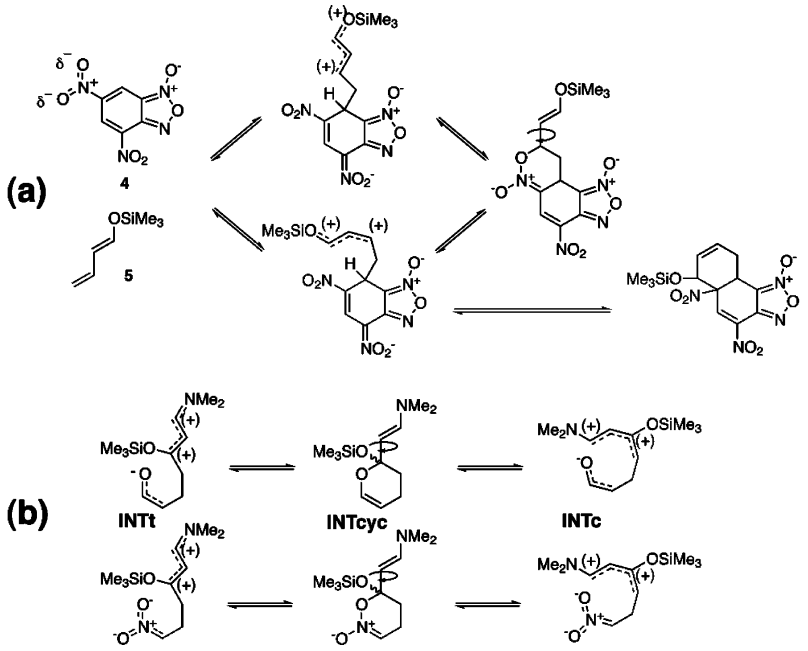

[a](a) The stepwise Diels–Alder reaction, involving isomerization *via* a heterocyclic intermediate, between 4,6-dinitrobenzofuroxan **4** and 1-trimethylsiloxy-1,3-butadiene **5**.[17,20] (b) An analogous isomerization between **1** and **2a** or **2b** (top and bottom respectively). The (+) signs indicate possible loci of positive charge due to resonance stabilization.

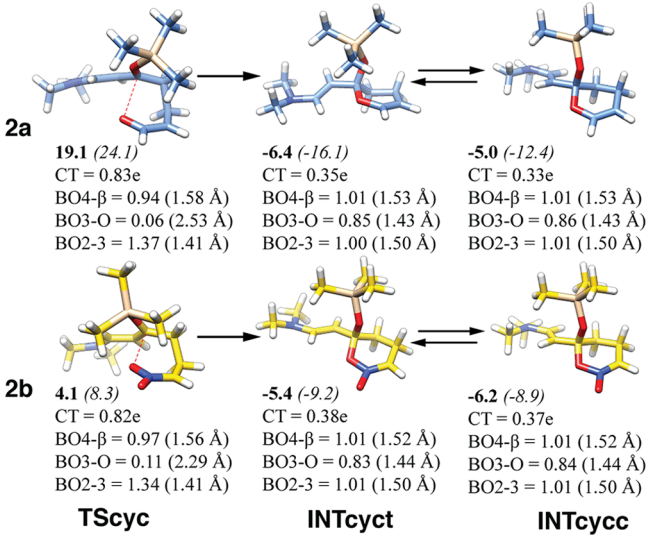

Figure 3. Free energies (with respect to separated reactants) and NBO-derived properties of the investigated heterocyclic species. Values in boldface and italics are ΔG at the SMD-M06-2X/6-311++G(2d,2p) and M06-2X/6-31+G(d) levels, respectively. Atom numbering refers to Scheme 2.

dinitrobiphenylene-1,8-diol **6**.[52] The dienophile–catalyst complex **2a**·**6** separated from the diene **1** is taken as the reference state. Selected geometries and NBO-derived properties are shown in Figure 4, and energies are reported in Table 4.[55]

As expected, $\Delta G^{\ddagger}$ is lowered for all three pathways. The preference for **TS1-DA** is virtually extinguished as the three TSs now have almost the same energy, and as seen from Table 4, there are no signs of a concerted mechanism in **TS1-DA**; the C_1–C_α distance is >4 Å. This strongly suggests a stepwise pathway proceeding to **INTprox** before passing over **TS2**. Furthermore, the zwitterionic intermediates are significantly stabilized with respect to both reactants and the second barrier, compared to the uncatalyzed system. Somewhat surprisingly, **INTc** and **INTt** are now both lower than **INTprox** by ∼2 kcal/mol in solvent. Thus, catalysis seems to promote (i) a stepwise reaction pathway and (ii) the persistence of any zwitterionic intermediate. We note the apparent long-range interactions between diene and catalyst, causing a close to perpendicular alignment of **6** to the intermediates and **TS1t** in Table 4. This could be an artifact of the gas-phase optimization (which tends to maximize the number of contacts). From the previous comparison, however, we rely on the single-point energies being sufficiently close to those derived from a solvent optimization.

The net catalytic effect of using **6** is −5.0 kcal/mol, which is about as good as it gets using H-bond catalysis (neglecting the dienophile-catalyst complexation equilibrium).[8] The catalytic effect is expected to decrease overall with increased solvent polarity, although it could lead to a distinct preference for the stepwise mechanism in the catalyzed reaction.

3.6. Generality of the Mechanism. Rawal's diene **1** is one of the most reactive dienes used in synthetic Diels–Alder chemistry, and to test the generality of the results found herein we addressed the reaction **2c** with four dienes **5a–d** of varying nucleophilicity (Scheme 4b). We focused on the "normal" reaction channel and thus calculated **TS1-DA**, **INTprox**, and **TS2**. The two latter states could not be found with regular gas-phase calculations but required a solvation model during optimization. The 6-311++G(2d,2p) free energies are given in Table 5, and we note a decreasing stability of the intermediate with decreasing $\Delta\omega$. Nevertheless, all reactions except **5a** + **2c** are formally stepwise. Although there is a qualitative correlation, one cannot directly relate the relative preference for a stepwise pathway to $\Delta\omega$. When comparing to the values in Table 2, we see that according to this classification the **1** + **2a**

dx.doi.org/10.1021/jo301176t | J. Org. Chem. 2012, 77, 6563–6573

Scheme 4[a]

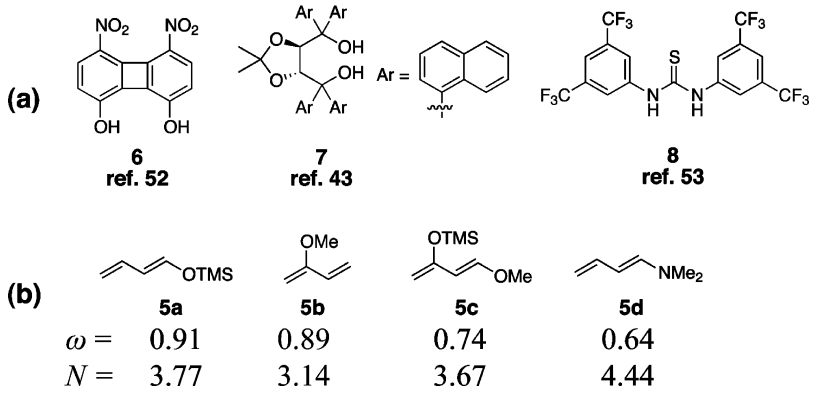

[a](a) Example of Diels–Alder organocatalysts stabilizing the TSs by H-bond donation. (b) Additional activated nucleophilic dienes. Global electrophilicity and nucleophilicity indices at the gas-phase M06-2X/6-31+G(d) level are indicated.

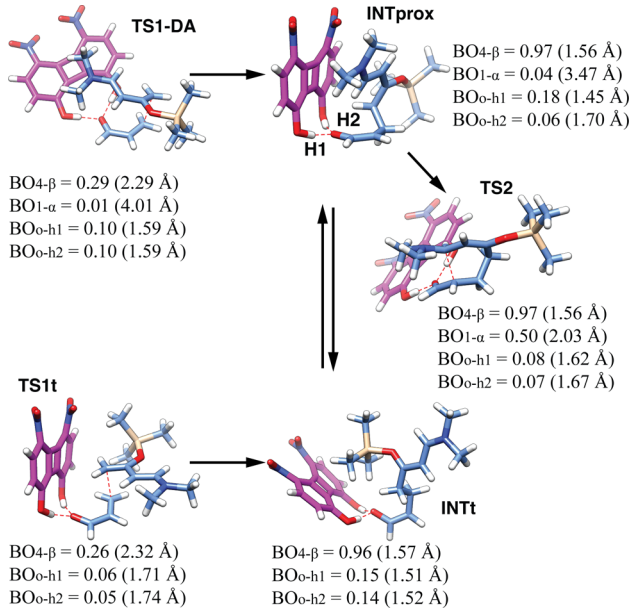

Figure 4. Selected states on the **1** + **2a**·**6** PES. The equilibrium arrows between **INTt** and **INTprox** indicate the possibility of isomerization *via* heterocyclic intermediates.

Table 4. M06-2X Free Energies of the 1+2a·6 System[a]

	6-31+G(d)		6-311++G(2d,2p)[b]	
state	ΔG_{cat}	$\Delta G_{cat-uncat}$	ΔG_{cat}	$\Delta G_{cat-uncat}$
TS1-DA	9.8	−11.5	16.2	−5.0
TS1c	11.5	−16.5	16.2	−10.6
TS1t	10.4	−14.8	16.4	−8.1
INTc	−7.8	−33.4	−7.6	−21.4
INTt	−2.9	−30.0	−7.6	−20.5
INTprox	−12.0	−26.8	−5.4	−13.7
TS2	−2.3	−14.5	4.1	−7.3

[a]All energies are given in kcal/mol. Thermodynamic corrections have been calculated at the level of optimization. [b]Including the SMD-PCM solvent model and a 1.89 kcal/mol standard state correction.

system is less activated than **5b** + **2c**, yet the second barrier is larger (*cf.* Table 2). Likewise, there is only a weak correlation between the nucleophilicity index[7] of the dienes and the height of the first and second barriers. These findings indicate that the

Table 5. M06-2X Free Energies of the 5 + 2c Systems[a]

state	**5a** $\Delta\omega$ = 1.00	**5b** $\Delta\omega$ = 1.02	**5c** $\Delta\omega$ = 1.17	**5d** $\Delta\omega$ = 1.28
TS1-DA	18.2	15.1	10.6	9.1
INTprox		9.2	−2.4	−9.8
TS2	10.3	10.6	1.5	−4.7

[a]All energies are at the SMD-PCM–M06-2X/6-311++G(2d,2p) level and are given in kcal/mol. Optimization was performed at the SMD-PCM–M062X/6-31+G(d) level. Thermodynamic corrections have been calculated at the level of optimization. A 1.89 kcal/mol standard state correction is included.

systems' overall ability to support excess charge in the TS and intermediates are likely more important for their relative stability than some absolute reactivity measure.

3.7. Intermediate Persistence and Implications for Organic Synthesis. The **4** + **5** intermediate studied by Lakhdar et al. was detected at −40 °C,[20] and our calculations predicted a kinetic stability of ∼10.5 kcal/mol using SMD-PCM–M06-2X/6-31++G(2d,2p).[17] In a subsequent paper Terrier and colleagues investigated a similar reaction that was predicted to be stepwise, but for which no intermediate was experimentally detected.[56] We found that the barrier between the lowest intermediate and **TS2** of this system was 6.3 kcal/mol, and hence we have a sense of what barrier height is required in order to accumulate traceable amounts of intermediate species (albeit under cryogenic conditions). We note that the SCS-MP2 method predicted lower relative stabilities for the intermediates, in concert with what we find in this study for the **1** + **2c** system (Table 3), but those results did not explain the experimental findings by Lakhdar et al.[17]

Using these results as benchmarks, we can conclude from the energies in Table 2 that the only two reactions in this study are likely to yield intermediates persistent enough for detection are the ones of **2c** and **2d**. Indeed, the results imply that the second step is rate-determining for these reactions. Furthermore, they proceed dominantly *via* **TS1t** and result in the accumulation of **INTt**. The backward reaction, which corresponds to the lowest pathway for depletion of **INTt**, has a barrier of 18.8 and 17.9 kcal/mol for **2c** and **2d**, respectively. In the case of **2d**, **TS1t** is only 2.3 kcal/mol lower in energy than **TS1-DA**, and thus the preference for the **TS1t**-pathway is within the limits of accuracy of the prediction. Although the calculated **INTcyc** of **2a** and **2b** are relatively stable with respect to the zwitterionic intermediates, the dominant **TS1-DA** channel is favored over

dx.doi.org/10.1021/jo301176t | J. Org. Chem. 2012, 77, 6563–6573

the formation of heterocyclic intermediates. In the case of **2b** it is difficult to predict the exact outcome, since **TS1-DA** is only 1.5 kcal/mol lower in energy than **TS1t**.

When a catalyst is applied, the **TS1t** and **TS1c** channels apparently become significant even for the moderately activated **1** + **2a** system. The three initial TSs are essentially equivalent and can all yield the product **3** through rapid interconversion of intermediates. The calculated energies of the **6**-catalyzed reaction coordinate furthermore suggest a significant stability of intermediates. Our results predict a second barrier of at least 9.5 kcal/mol (this is assuming the initial **TS1-DA** channel and no formation of a cyclic intermediate). Hence, the **1** + **2a**·**6** system is within or close to the limit for detection.

Apart from the fundamental interest from a mechanistic point of view, determining whether a Diels–Alder reaction is concerted or stepwise can be important for making predictions about possible stereochemical outcomes. We have previously used B3LYP to investigate the possibility of a proton shift, leading to a (undesired) Michael-type adduct, but found the barrier to be insurmountable.[8] Given the toolbox presented in this work, it may however be worthwhile to revisit this possibility. Perhaps a more central issue is the possibility of rotation of the C_α–C_β bond in the intermediates, which could lead to the second bond forming on the opposite face of the dienophile. A third aspect of our results is the catalytic promotion of the stepwise pathway, which could perhaps be exploited to design more efficient organocatalysts or enzymes,[24,57] with potentially new stereochemical targets.

4. CONCLUSIONS

We find stepwise Diels–Alder reaction to be a quite general concept applicable to a broad range of activated reactants. All three reaction channels studied for the **1**+**2a**–**d** additions are two-step mechanisms and can formally be regarded as nucleophilic additions followed by ring closure. They can be said to behave much like Lewis acid catalyzed reactions of less activated reactants.[15,51] The preference for a stepwise pathway depends on both the reactants' and solvent's ability to stabilize the charge separation. The conjugate addition-like TSs **TS1c** and **TS1t** are increasingly favored compared to the Diels–Alder-like conformation **TS1-DA** with more electrophilic dienophiles. For the most activated species, the *trans* pathway is the most favored, but there is no possible *trans-cis* isomerization route for the intermediates unless an alternative, temporary cycloadduct is formed. Such intermediate species were found for the carbonyl and nitro dienophiles **2a** and **2b** but not for the cyano-substituted **2c** and **2d**. Most intermediates found in this work are transient due to a low second barrier, but on the basis of earlier work[17,20,56] it should be possible to detect intermediates of the reaction and between the **1** + **2c** and **1** + **2d** systems and possibly the **6**-catalyzed **1** + **2a** reaction. In the latter system, we saw a dramatic increase in the preference of the stepwise channels upon adding a catalyst, as well as improved intermediate stabilization. Compared to experimental work by, e.g., Rawal and co-workers,[43] we see that the putative organocatalyzed Diels–Alder reactions between **1** and **2a** should be regarded as stepwise additions, although the exact mechanistic preference remains somewhat veiled.[58]

Finally, we conclude that B3LYP tends to overestimate the nucleophilic addition character of these reactions, leading to exaggerated asynchronicity and a low preference for the **TS1-DA** pathway. M06-2X predicts lower barriers and intermediate energies than the SCS-MP2 method, but the overall shapes of the energy landscape are similar.

■ ASSOCIATED CONTENT

Supporting Information

Additional data, figures, an extended discussion on basis set and correlations with molecular properties, as well as optimized M06-2X geometries of all species mentioned in the text. This information is available free of charge via the Internet at http://pubs.acs.org.

■ AUTHOR INFORMATION

Corresponding Author

*E-mail: tore@physchem.kth.se.

Notes

The authors declare no competing financial interest.

■ ACKNOWLEDGMENTS

This work has been financed by the Cambridge Crystallographic Data Centre (CCDC) and the Swedish Research Council (VR).

■ REFERENCES

(1) Diels, O.; Alder, K. *Justus Liebigs Ann. Chem.* **1928**, *460*, 98.
(2) Houk, K. N.; Gonzalez, J.; Li, Y. *Acc. Chem. Res.* **1995**, *28*, 81–90.
(3) Cheong, P. H.-Y.; Legault, C. Y.; Um, J. M.; Celebi-Ölcüm, N.; Houk, K. N. *Chem. Rev.* **2011**, *111*, 5042–5137.
(4) Schreiner, P. R. *Chem. Soc. Rev.* **2003**, *32*, 289–296.
(5) Zhang, Z.; Schreiner, P. R. *Chem. Soc. Rev.* **2009**, *38*, 1187–1198.
(6) Domingo, L. R.; Saéz, J. A. *Org. Biomol. Chem.* **2009**, *7*, 3576–3583.
(7) Domingo, L. R.; Chamorro, E.; Pérez, P. *J. Org. Chem.* **2008**, *73*, 4615–4624.
(8) Linder, M.; Brinck, T. *Org. Biomol. Chem.* **2009**, *7*, 1304–1311.
(9) Rooshenas, P.; Hof, K.; Schreiner, P. R.; Williams, C. M. *Eur. J. Org. Chem.* **2011**, *2011*, 983–992.
(10) Goldstein, E.; Beno, B.; Houk, K. *J. Am. Chem. Soc.* **1996**, *118*, 6036–6043.
(11) A recent electron localization function (ELF) analysis by Domingo and colleagues[59] indicates a "pseudoradical" nature even of concerted non-polar TSs (Scheme 1a). This analysis is reasonable considering the symmetry of the standard butadiene-ethylene system, but once the symmetry is broken, e.g., by an activating group), the net electron flow is directional. Hence the general mechanism in Scheme 1b is the most viable description in the majority of reactions (polar Diels–Alder in the terminology of Domingo[6]).
(12) Domingo, L. R.; Aurell, M. J.; Pérez, P.; Contreras, R. *J. Phys. Chem. A* **2002**, *106*, 6871–6875.
(13) Domingo, L. R.; Arnó, M.; Contreras, R.; Pérez, P. *J. Phys. Chem. A* **2002**, *106*, 952–961.
(14) (a) Domingo, L. R.; Andrés, J. *J. Org. Chem.* **2003**, *68*, 8662–8668. (b) Polo, V.; Domingo, L. R.; Andrés, J. *J. Phys. Chem. A* **2005**, *109*, 10438–10444.
(15) (a) Domingo, L. R.; Andrés, J.; Alves, C. N. *Eur. J. Org. Chem.* **2002**, *2002*, 2557–2564. (b) Gordillo, R.; Dudding, T.; Anderson, C.; Houk, K. *Org. Lett.* **2007**, *9*, 501–503.
(16) (a) Celebi-Ölcüm, N.; Ess, D. H.; Aviyente, V.; Houk, K. N. *J. Am. Chem. Soc.* **2007**, *129*, 4528–4529. (b) Ess, D.; Wheeler, S.; Iafe, R.; Xu, L.; Celebi-Ölcüm, N.; Houk, K. *Angew. Chem., Int. Ed.* **2008**, *47*, 7592–7601.
(17) Linder, M.; Johansson, A. J.; Brinck, T. *Org. Lett.* **2012**, *14*, 118–121.
(18) Woodward, R. B.; Hoffmann, R. *Angew. Chem., Int. Ed. Engl.* **1969**, *8*, 781.
(19) Gompper, R. *Angew. Chem., Int. Ed.* **1969**, *8*, 312–327.

(20) Lakhdar, S.; Terrier, F.; Vichard, D.; Berionni, G.; El Guesmi, N.; Goumont, R.; Boubaker, T. *Chem.—Eur. J.* **2010**, *16*, 5681−5690.
(21) Pieniazek, S.; Clemente, F.; Houk, K. *Angew. Chem., Int. Ed.* **2008**, *47*, 7746−7746.
(22) (a) Zhao, Y.; Schultz, N. E.; Truhlar, D. G. *J. Chem. Phys.* **2005**, *123*, 161103. (b) Zhao, Y.; Schultz, N. E.; Truhlar, D. G. *J. Chem. Theory Comput.* **2006**, *2*, 364−382. (c) Zhao, Y.; Truhlar, D. G. *J. Chem. Phys.* **2006**, *125*, 194101.
(23) Zhao, Y.; Truhlar, D. G. *Theor. Chem. Acc.* **2008**, *120*, 215−241.
(24) Linder, M.; Johansson, A. J.; Manta, B.; Olsson, P.; Brinck, T. *Chem. Commun.* **2012**, *48*, 5665−5667.
(25) (a) Becke, A. D. *Phys. Rev. A* **1988**, *38*, 3098−3100. (b) Becke, A. D. *J. Chem. Phys.* **1993**, *98*, 1372−1377. (c) Lee, C.; Yang, W.; Parr, R. G. *Phys. Rev. B* **1988**, *37*, 785−789.
(26) Simón, L.; Goodman, J. M. *Org. Biomol. Chem.* **2011**, *9*, 689−700.
(27) Grimme, S. *J. Comput. Chem.* **2004**, *25*, 1463−1473.
(28) Grimme, S.; Steinmetz, M.; Korth, M. *J. Org. Chem.* **2007**, *72*, 2118−2126.
(29) Goumans, T. P. M.; Ehlers, A. W.; Lammertsma, K.; Würthwein, E.-U.; Grimme, S. *Chem.—Eur. J.* **2004**, *10*, 6468−6475.
(30) Grimme, S.; Muck-Lichtenfeld, C.; Wurthwein, E.-U.; Ehlers, A.; Goumans, T.; Lammertsma, K. *J. Phys. Chem. A* **2006**, *110*, 2583−2586.
(31) Hohenstein, E. G.; Chill, S. T.; Sherrill, C. D. *J. Chem. Theory Comput.* **2008**, *4*, 1996−2000.
(32) Rayne, S.; Forest, K. Performance of the M062X density functional against the ISOL set of benchmark isomerization energies for large organic molecules, 2010; available online at http://dx.doi.org/10.1038/npre.2010.5183.1.
(33) Møller, C.; Plesset, M. S. *Phys. Rev.* **1934**, *46*, 618−622.
(34) Grimme, S. *J. Chem. Phys.* **2003**, *118*, 9095−9102.
(35) Zhao, Y.; Truhlar, D. G. *Chem. Phys. Lett.* **2011**, *502*, 1−13.
(36) (a) Gu, J.; Wang, J.; Leszczynski, J.; Xie, Y.; H., F. S., III *Chem. Phys. Lett.* **2008**, *459*, 164−166. (b) Garr, A. N.; Luo, D.; Brown, N.; Cramer, C. J.; Buszek, K. R.; VanderVelde, D. *Org. Lett.* **2010**, *12*, 96−99. (c) Tang, S.-Y.; Shi, J.; Guo, Q.-X. *Org. Biomol. Chem.* **2012**, *10*, 2673−2682. (d) Pham, H. V.; Martin, D. B. C.; Vanderwal, C. D.; Houk, K. N. *Chem. Sci.* **2012**, *3*, 1650−1655.
(37) Ditchfield, R.; Hehre, W. J.; Pople, J. A. *J. Chem. Phys.* **1971**, *54*, 724−728.
(38) (a) Barone, V.; Cossi, M. *J. Phys. Chem. A* **1998**, *102*, 1995−2001. (b) Cossi, M.; Rega, N.; Scalmani, G.; Barone, V. *J. Comput. Chem.* **2003**, *24*, 669−681. (c) Marenich, A. V.; Cramer, C. J.; Truhlar, D. G. *J. Phys. Chem. B* **2009**, *113*, 6378−6396.
(39) Frisch, M. J. et al. *Gaussian 09, Revision A.02*; Gaussian Inc.: Wallingford, CT, 2009.
(40) Wheeler, S. E.; Houk, K. N. *J. Chem. Theory Comput.* **2010**, *6*, 395−404.
(41) Wiberg, K. B. *Tetrahedron* **1968**, *24*, 1083−1096.
(42) (a) Reed, A. E.; Weinstock, R. B.; Weinhold, F. *J. Chem. Phys.* **1985**, *83*, 735−746. (b) Reed, A. E.; Curtiss, L. A.; Weinhold, F. *Chem. Rev.* **1988**, *88*, 899−895.
(43) (a) Huang, Y.; Unni, A. K.; Thadani, A. N.; Rawal, V. H. *Nature* **2003**, *424*, 146−146. (b) N. Thadani, A.; R. Stankovic, A.; H. Rawal, V. *Proc. Natl. Acad. Sci. U.S.A.* **2004**, *101*, 5846−5850.
(44) Parr, R. G.; Szentpály, L.; Liu, S. *J. Am. Chem. Soc.* **1999**, *121*, 1922−1924.
(45) (a) Parr, R. G.; Pearson, R. G. *J. Am. Chem. Soc.* **1983**, *105*, 7512−7516. (b) Parr, R. G.; Chattaraj, P. K. *J. Am. Chem. Soc.* **1991**, *113*, 1854−1855.
(46) Domingo, L. R.; Aurell, M. J.; Pérez, P.; Contreras, R. *Tetrahedron* **2002**, *58*, 4417−4423.
(47) Li, Z.-M.; Wang, Q.-R. *Int. J. Quantum Chem.* **2011**, *111*, 3805−3815.
(48) Schreiner, P. R.; Chernish, L. V.; Gunchenko, P. A.; Tikhonchuk, E. Y.; Hausmann, H.; Serafin, M.; Schlecht, S.; Dahl, J. E. P.; Carlson, R. M. K.; Fokin, A. A. *Nature* **2011**, *477*, 308−311.
(49) (a) Gonzalez, C.; Schlegel, H. B. *J. Chem. Phys.* **1989**, *90*, 2154−2161. (b) Gonzalez, C.; Schlegel, H. B. *J. Phys. Chem.* **1990**, *94*, 5523−5527.
(50) Kong, S.; Evanseck, J. *J. Am. Chem. Soc.* **2000**, *122*, 10418−10427.
(51) Yamabe, S.; Minato, T. *J. Org. Chem.* **2000**, *65*, 1830−1841.
(52) Kelly, T.; Meghani, P.; Ekkundi, V. S. *Tetrahedron Lett.* **1991**, *31*, 3381.
(53) (a) Schreiner, P.; Wittkopp, A. *Org. Lett.* **2002**, *4*, 217−220. (b) Wittkopp, A.; Schreiner, P. R. *Chem.—Eur. J.* **2003**, *9*, 407−414.
(54) (a) Gioia, C.; Hauville, A.; Bernardi, L.; Fini, F.; Ricci, A. *Angew. Chem., Int. Ed.* **2008**, *47*, 9236−9239. (b) Ishihara, K.; Nakano, K.; Akakura, M. *Org. Lett.* **2008**, *10*, 2893−2896. (c) Kano, T.; Tanaka, Y.; Osawa, K.; Yurino, T.; Maruoka, K. *Chem. Comm* **2009**, *15*, 1956−1958.
(55) We note that for a dieneophile−diol complex, several binding modes are possible.[3] In this work, we have chosen to treat only the bidentate mode since it was found to be the most stable for **2a·6**.
(56) Steglenko, D. V.; Kletsky, M. E.; Kurbatov, S. V.; Tatarov, A. V.; Minkin, V. I.; Goumont, R.; Terrier, F. *Chem.—Eur. J.* **2011**, *17*, 7592−7604.
(57) (a) Siegel, J. B.; Zanghellini, A.; Lovick, H. M.; Kiss, G.; Lambert, A. R.; St.Clair, J. L.; Gallaher, J. L.; Hilvert, D.; Gelb, M. H.; Stoddard, B. L.; Houk, K. N.; Michael, F. E.; Baker, D. *Science* **2010**, *329*, 309−313. (b) Linder, M.; Johansson, A. J.; Olsson, T. S. G.; Liebeschuetz, J.; Brinck, T. *J. Chem. Inf. Model.* **2011**, *51*, 1906−1917.
(58) While this paper was in review, an article by Pham et al. was published (ref 36d), in which the authors demonstrate that an intramolecular, IED Diels−Alder reaction is a stepwise process. Notably, the authors aptly describe a "mechanistic continuum" spanning between concerted synchronous and fully stepwise pathways which is perfectly in line with the conclusions drawn in this study.
(59) Domingo, L. R.; Chamorro, E.; Pérez, P. *Org. Biomol. Chem.* **2010**, *8*, 5495−5504.